Linear Copolymer Analysis with Dual-Detection Size Exclusion Chromatography: Correction for Instrumental Broadening

R. O. BIELSA and G. R. MEIRA*

INTEC (CONICET and Universidad Nacional del Litoral), C.C. 91, 3000 Santa Fe, Argentina

SYNOPSIS

This article deals with data treatment problems associated with the estimation of the combined distribution of molecular weights and chemical composition in linear copolymers by size exclusion chromatography, when correction for instrumental broadening is considered. Standard dual detection is assumed, i.e., the chromatograph is fitted with a "universal" detector (a differential refractometer) and a specific sensor to one comonomer only (a UV spectrophotometer). A real and a "synthetic" example (involving the analysis of a diblock styrene–butadiene rubber) are presented. Also, a propagation of errors study associated with the deconvolution operations is developed. It is concluded that the best calculation procedure is to first compute the combined distributions from the raw chromatograms and then correct such distributions for instrumental broadening. © 1992 John Wiley & Sons, Inc.

INTRODUCTION

Size exclusion chromatography (SEC) is presently the most important analytical tool for estimating the combined distribution of molecular weights and chemical composition in linear copolymers. This is because for many copolymers standard dual detection (i.e., UV spectroscopy plus differential refractometry) allows the determination of the instantaneous mass and average composition at each retention time.[1-10] Consider a linear copolymer with repeating units S and B. Also, assume that while the UV spectrophotometer senses component S only the differential refractometer responds to the two comonomers. In the ideal case of no instrumental or other broadening effects, the following detector equations may be written[8-10]:

$$A(i) = k\,p(i)G(i) \tag{1}$$

$$n(i) = \{\nu_S p(i) + \nu_B[1 - p(i)]\}G(i) \tag{2}$$

where i is the elution time or elution volume; $A(i)$, $n(i)$ are the baseline-corrected chromatograms, corresponding to the absorbance and refractive index detectors, respectively; $G(i)$ is the mass-elution time distribution; $p(i)$ is the composition (weight fraction of S)-elution time distribution; and k, ν_S, and ν_B are constants that can be estimated by calibration. From eqs. (1) and (2), the elution time distributions may be calculated as follows:

$$p(i) = \frac{\nu_B[A(i)/n(i)]}{k + (\nu_B - \nu_S)[A(i)/n(i)]} \tag{3}$$

$$G(i) = \frac{n(i)}{\nu_B} + \frac{(\nu_B - \nu_S)}{k\nu_B}A(i) \tag{4}$$

Equation (4) is numerically well conditioned because it consists of two terms, each linear in the measurements $n(i)$ and $A(i)$. This is not the case of eq. (3), however, where problems are to be expected for low values of $n(i)$. From eqs. (3) and (4), García-Rubio[10] developed the following expressions regarding the propagation of errors into the distributions due to variations in the measurements:

$$\mathrm{var}[p(i)] = \left[\frac{\nu_B k}{n(i)}\right]^2 \times \frac{\mathrm{var}[A(i)] + [A(i)/n(i)]^2\mathrm{var}[n(i)]}{\{k + (\nu_B - \nu_S)[A(i)/n(i)]\}^4} \tag{5}$$

* To whom correspondence should be addressed.

Journal of Applied Polymer Science, Vol. 46, 835–845 (1992)
 CCC 0021-8995/92/050835-11

$$\text{var}[G(i)] = \frac{\text{var}[n(i)]}{v_B^2} + \frac{(v_B - v_S)^2}{(kv_B)^2}\text{var}[A(i)] \quad (6)$$

where var[.] indicates time-varying variance of [.].

Instrumental broadening correction is important when narrow-distributed copolymers are analyzed or when fine details of the combined molecular weight/chemical composition distribution are required. In dual-detection SEC, this correction has been theoretically investigated in a previous publication,[8] and the main conclusions of that work were: (1) the instrumental broadening functions associated to each chromatogram and to the uncorrected distributions $G'(i)$ and $p'(i)$ are all identical to the normal spreading function determined for linear homopolymers and mass detectors; and (2) instrumental broadening correction involves independent deconvolutions of the original chromatograms prior to applying eqs. (3) and (4) (correction 1) or independent deconvolutions of the elution time distributions obtained after directly processing the chromatograms through the said equations (correction 2). This is illustrated in Figure 1, where a primed variable indicates distortion by instrumental broadening, while an unprimed variable indicates that it has been corrected for such distortion.

Let $x(i)$ indistinctly represent $A(i)$, $n(i)$, $p(i)$, or $G(i)$. The following discrete and stochastic equivalent of Tung's equation[11] may be written to express the interrelationship between $x(i)$ and its broadened version $x'(i)$[12]:

$$x'(i) = \sum_{i_0=-c}^{i_0=d} h(i, i_0)x(i_0) + v_x(i) \qquad (i = 1, 2, \ldots, n) \quad (7)$$

where i and i_0 both represent discrete times (or volumes); $(-c, d)$ is a wide enough support that includes all nonzero values of $x'(i)$; $h(i, i_0)$ is the spreading function or normalized set of chromatograms of hypothetical monodisperse homopolymers with different mean elution times i_0; and $v_x(i)$ is an additive zero-mean measurement noise of known variance. In vectorial notation, eq. (7) may be written

$$\mathbf{x}' = \mathbf{H}\mathbf{x} + \mathbf{v}_x \quad (8)$$

where $\mathbf{H}$ is a matrix and $\mathbf{x}'$, $\mathbf{x}$, and $\mathbf{v}_x$ are column vectors. Several deconvolution techniques that allow the calculation of $\mathbf{x}$ from the knowledge of $\mathbf{x}'$ and $\mathbf{H}$ have been compared in Ref. 12.

If the elution time distributions $G(i)$ and $p(i)$ are known, then the global weight fraction of S in the copolymer ($\bar{p}_S$) can be directly calculated from

$$\bar{p}_S = \frac{\sum G(i)p(i)}{\sum G(i)} \quad (9)$$

To obtain the distributions of molecular weights $G(M)$, and of chemical composition $G(p)$, the calibration $M(i)$ is further required. The transformation of $G(i)$ into a continuous $G(M)$ function with a linear M involves appropriate modifications of the heights in addition to modifications of the horizontal axis.[10] The number- and weight-average molecular weights are obtained from $G(M)$ [or from $G(i)$ and $M(i)$] in the normal fashion, i.e.

$$M_n = \frac{\sum G(i)}{\sum [G(i)/M(i)]} = \frac{\sum G(M)}{\sum [G(M)/M]} \quad (10)$$

$$M_w = \frac{\sum G(i)M(i)}{\sum G(i)} = \frac{\sum G(M)M}{\sum G(M)} \quad (11)$$

Note that if $G(M)$ is utilized in eqs. (10) and (11) then equally spaced points along M must be considered; and, compared to the direct calculation via $G(i)$ and $M(i)$, larger errors are to be expected.

This work aims at evaluating the calculation paths illustrated in Figure 1. Such paths are tested on a "real" and a "synthetic" example, corresponding to the analysis of a styrene–butadiene rubber (SBR). For the synthetic example, two possible "measurement" models are proposed. A propagation of errors study for the corrections in Figure 1 is developed. To this effect, eqs. (5) and (6) are used in series with a new expression that provides a crude estimation of the deconvolution errors. The errors related to the calculation of $G(M)$ and $p(M)$ from the elution time distributions are not investigated in this work.

MEASUREMENT MODELS

Synthetic examples with *a priori* known solutions are sometimes ideal to test alternative numerical procedures. To this effect, the measurement models must be relatively accurate compared to the inversion or correction procedures. This is verified in our case, where such models involve a series combination of the relatively simple multiplicative eqs. (1) and

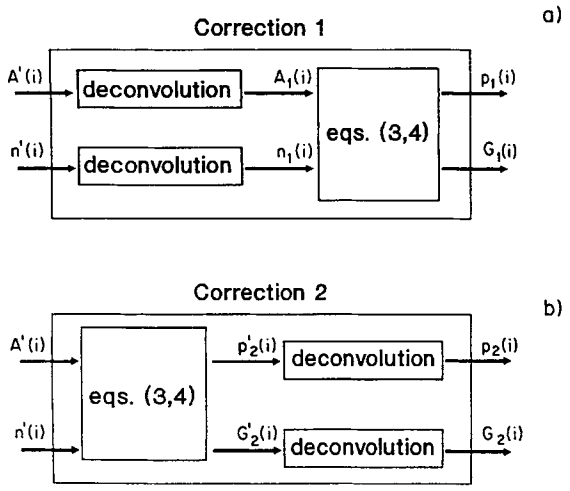

Figure 1 Calculation of the mass-elution time and composition-elution time distributions. (a) Correction 1. (b) Correction 2.

(2) together with the well-behaved convolution operations of eq. (8). According to the order of such computations, the models represented in Figure 2 are possible.

In model 1, the zero-mean white noises $v_A(i)$ and $v_n(i)$ are added to the noise-free (but distorted) measurements $A''(i)$ and $n''(i)$. In model 2, the zero-mean white noises $v_p(i)$ and $v_G(i)$ are added to the noise-free (but distorted) distributions $p''(i)$ and $G''(i)$ to associate the additive noises with the convolution models, as in eq. (7). The variances of $v_A(i)$ and $v_n(i)$ may be assumed time invariant and can be estimated from the baselines before and after the chromatogram peaks.[13] The variances of $v_p(i)$ and $v_G(i)$ may also be assumed time invariant and can be estimated from $\text{var}[v_A(i)]$, $\text{var}[v_n(i)]$, and eqs. (3) and (4).

The nonlinear block of eqs. (1) and (2) generate path-dependent solutions and therefore different inputs are to be expected from each of the two models. Inversion operations provide better results when they are performed in reverse order with respect to the synthesis procedure. Thus, correction 1 is expected to perform better with the outputs of model 1, and the same is valid for correction 2 and model 2.

DECONVOLUTION ERRORS

Assume that $\mathbf{H}$ is a square matrix in eq. (8). Since $\mathbf{v}_x$ is zero-mean, an obvious estimation of $\mathbf{x}$ is obtained through

$$\hat{\mathbf{x}} = \mathbf{H}^{-1}\mathbf{x}' \tag{12}$$

Deconvolutions produced via eq. (12) are in general unacceptably oscillatory but are optimal in the sense that $\mathbf{H}\hat{\mathbf{x}}$ constitutes a good recuperation of $\mathbf{x}'$. Other deconvolution techniques[13,14] provide estimations that are closer to the "true" $\mathbf{x}$ function and are therefore preferable in practice. In what follows, a propagation of errors study is developed that is based upon the simple estimation of eq. (12).

Rewrite eq. (12) as follows:

$$x(i) = \sum_{i_0=1}^{n} f(i, i_0)x'(i_0) \quad (i = 1, 2, \ldots, n) \tag{13}$$

with

$$\mathbf{F} = \mathbf{H}^{-1} \tag{14}$$

where $f(i, i_0)$ is a generic element of resolvent matrix $\mathbf{F}$. To investigate the effect on $x(i)$ of independent variations of $f(i, i_0)$ and $x'(i)$, eq. (13) can be linearized by truncation of a Taylor's expansion around some appropriate true or reference functions (represented by subscript r), with the result

$$\tilde{x}(i) = \sum_{i_0=1}^{n} \left[\frac{\partial x(i)}{\partial f(i, i_0)}\right]_r \tilde{f}(i, i_0) + \sum_{i_0=1}^{n} \left[\frac{\partial x(i)}{\partial x'(i_0)}\right]_r \tilde{x}'(i_0) \quad (i = 1, 2, \ldots, n) \tag{15}$$

with

$$\tilde{f}(i, i_0) = f(i, i_0) - [f(i, i_0)]_r$$
$$\tilde{x}'(i) = x'(i) - [x'(i)]_r$$
$$\tilde{x}(i) = x(i) - [x(i)]_r$$

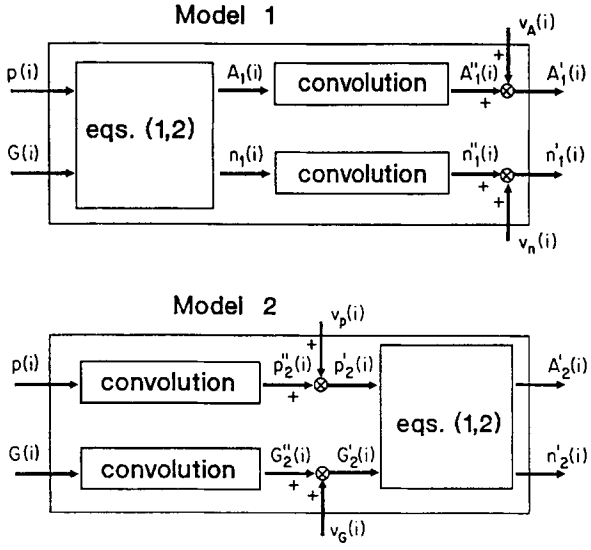

Figure 2 "Measurement" models for synthetic example.

From eqs. (13)–(15), one obtains

$$\tilde{x}(i) = \sum_{i_0=1}^{n} [x'(i_0)]_r \tilde{f}(i, i_0) + \sum_{i_0=1}^{n} [f(i, i_0)]_r \tilde{x}'(i_0) \quad (i = 1, 2, \ldots, n) \quad (16)$$

and application of operator var[.] to eq. (16) provides

$$\text{var}[\tilde{x}(i)] = \sum_{i_0=1}^{n} [x'(i_0)]_r^2 \text{var}[\tilde{f}(i, i_0)] + \sum_{i_0=1}^{n} [f(i, i_0)]_r^2 \text{var}[\tilde{x}'(i_0)] \quad (i = 1, 2, \ldots, n) \quad (17)$$

But, $\text{var}[\tilde{x}(i)] = \text{var}[x(i)]$, and similarly with the other difference variables. Therefore, eq. (17) results in

$$\text{var}[x(i)] = \sum_{i_0=1}^{n} [x'(i_0)]_r^2 \text{var}[f(i, i_0)] + \sum_{i_0=1}^{n} [f(i, i_0)]_r^2 \text{var}[x'(i_0)] \quad (i = 1, 2, \ldots, n) \quad (18)$$

For the propagation of errors associated with the first step of correction 1, eq. (18) yields

$$\text{var}[A_1(i)] = \sum_{i_0=1}^{n} [A'(i_0)]_r^2 \text{var}[f(i, i_0)] + \sum_{i_0=1}^{n} [f(i, i_0)]_r^2 \text{var}[A'(i_0)] \quad (i = 1, 2, \ldots, n) \quad (19)$$

$$\text{var}[n_1(i)] = \sum_{i_0=1}^{n} [n'(i_0)]_r^2 \text{var}[f(i, i_0)] + \sum_{i_0=1}^{n} [f(i, i_0)]_r^2 \text{var}[n'(i_0)] \quad (i = 1, 2, \ldots, n) \quad (20)$$

Similarly, for the second step of correction 2 the following may be written:

$$\text{var}[p_2(i)] = \sum_{i_0=1}^{n} [p_2'(i_0)]_r^2 \text{var}[f(i, i_0)] + \sum_{i_0=1}^{n} [f(i, i_0)]_r^2 \text{var}[p_2'(i_0)] \quad (i = 1, 2, \ldots, n) \quad (21)$$

$$\text{var}[G_2(i)] = \sum_{i_0=1}^{n} [G_2'(i_0)]_r^2 \text{var}[f(i, i_0)] + \sum_{i_0=1}^{n} [f(i, i_0)]_r^2 \text{var}[G_2'(i_0)] \quad (i = 1, 2, \ldots, n) \quad (22)$$

In eqs. (19) and (20), $\text{var}[A'(i)]$ and $\text{var}[n'(i)]$ could be estimated from a statistically significant set of measurements $A'(i)$ and $n'(i)$ of a given copolymer sample. In eqs. (21) and (22), $\text{var}[p_2'(i)]$ and $\text{var}[G_2'(i)]$ could be obtained from eqs. (5) and (6), with $A(i)$ and $n(i)$ replaced by their corresponding primed variables.

For estimating $\text{var}[f(i, i_0)]$ in eqs. (19)–(22), remember that matrix $\mathbf{F}$ is related to the inverse of $\mathbf{H}$. The files of $\mathbf{H}$ contain the spreading functions at the different mean retention times i_0. Therefore, all elements of $\mathbf{H}$ are lower than unity, with the maxima in the diagonal. Since the transformation of $\mathbf{H}$ into $\mathbf{H}^{-1}$ involves a highly nonlinear combination of all elements of $\mathbf{H}$; the propagation of errors due to variations in the elements of $\mathbf{H}^{-1}$ is extremely complicated to develop. For this reason, the following approximation of $\mathbf{H}^{-1}$ will be utilized (see Appendix):

$$\mathbf{F} = \mathbf{H}^{-1} \cong 2\mathbf{I} - \mathbf{H} \quad (23)$$

where $\mathbf{I}$ is the identity matrix. Application of var[.] to each element of eq. (23) provides

$$\text{var}[f(i, i_0)] \cong \text{var}[h(i, i_0)] \quad (24)$$

where $h(i, i_0)$ is a generic element of $\mathbf{H}$. Thus, one can replace $\text{var}[f(i, i_0)]$ for $\text{var}[h(i, i_0)]$ in eqs. (19)–(22). Ultimately, $\text{var}[h(i, i_0)]$ will depend upon the detector errors and upon the techniques applied for the spreading function determination. Note that with the simplification of eq. (24) the truncation errors accumulated in the inversion of $\mathbf{H}$ are not contemplated in eqs. (19)–(22). Since eqs. (13), (14), and (23) only provide crude estimations of $\mathbf{x}$, then it is to be expected that the confidence limits determined through eqs. (19)–(22) and (24)

should constitute upper bounds for other more accurate deconvolutions techniques.[13,14]

EVALUATION EXAMPLES

Experimental Work

Consider the analysis of a narrow-distributed diblock SBR that was synthesized anionically as follows. First, the polybutadiene (PB) block was produced and a sample of such polymer was taken. Then, the styrene block was generated on the remaining "living" polymer, with a nominal 20% mass fraction of styrene in the final copolymer.

The calibrations that follow were employed in the synthetic as well as in the experimental example. All data analysis programs were written in FORTRAN 77 for a VAX 11/780 computer.

A Waters Assoc. (Milford, MA) ALC/GPC 244 size exclusion chromatograph was employed, fitted with the full set of (six) μ-Styragel columns, a Model 440 UV absorbance detector (set at 254 nm), and a Model R-401 differential refractometer (DR). The carrier solvent was tetrahydrofuran (THF) at 1 mL/min. The two detectors produced signals in the range 0–10 mV, and a 12-bit analog/digital converter translated such voltages into the range 0–4096. A Digital Minc 11 computer allowed the data acquisition. The digitalized data were then transfered to the VAX machine for baseline correction and remaining data processing. According to the injected sample, electronic zeroes and gains were adjusted to provide large but nonsaturated outputs. Then, the chromatogram heights were multiplied by the set attenuations to refer all measurements to the same basis. In all cases, toluene was added as internal standard to correct for solvent flow deviations.

Figure 3(a) represents the final digitalized chromatograms after rescaling with attenuations of 0.2 and 4 for the UV and DR detectors, respectively. The UV signal is shown shifted to account for the time lag between sensors.

For the *detector calibrations,* a polystyrene (PS) standard and the PB sample taken during the SBR synthesis were employed. The narrow PS standard (M_w = 19400 g/mol) was chosen as a similar mean elution time as the copolymer and the PB sample ensured that its microstructure coincided with that of the butadiene in the copolymer. The calibrations were performed as follows:

1. THF solutions (0.25 g/100 mL) of such homopolymers were prepared.
2. Chromatograms corresponding to injections of 25, 100, 250, and 500 μL of the said solutions were obtained and, as expected, the UV signal for the PB sample was practically null.
3. The areas under the chromatograms were plotted vs. the injected polymer masses and the experimental points fell rather well on straight lines. The slopes of such plots provided the sought calibrations, with the result

$$k = 25{,}800 \quad \nu_S = 272{,}300 \quad \nu_B = 223{,}500 \qquad (25)$$

Replacement of eqs. (25) into eqs. (3) and (4) determines that $G(i)$ is practically proportional to $n(i)$ while $p(i)$ is essentially proportional to the signals ratio $[A(i)/n(i)]$.

The *instrumental broadening calibration* was obtained by the recycle method proposed by Alba and Meira[15] and employing the previously mentioned PS standard. Due to the narrow elution range of the copolymer chromatograms, the instrumental broadening was assumed uniform; the final spreading function $h(i)$ is represented in Figure 3(b). Note that: (1) The breadth of $h(i)$ is similar to that of the measured chromatograms, thus justifying the broadening correction; and (2) $h(i)$ is positively skewed and therefore small shifts in the averages will be introduced by the convolution/deconvolution operations.

The *main calibration* was performed with sets of commercially available narrow PS and PB standards. Their peak molecular weights, which we shall call M_S and M_B, respectively, were obtained from $(M_n M_w)^{0.5}$. The individual calibrations resulted in

$$\log[M_S(i)] = -0.1821i + 12.8219 \qquad (26)$$

$$\log[M_B(i)] = -0.1821i + 12.5202 \qquad (27)$$

and the copolymer molecular weights $M(i)$ were found by the following interpolation[1]:

$$\log[M(i)] = p(i)\log[M_S(i)] + [1 - p(i)]\log[M_B(i)] \qquad (28)$$

Note that with eq. (28) the copolymer molecular weights depend upon $p(i)$.

Consider the estimation of the (constant) *variances of the zero-mean noises* $v_A(i)$, $v_n(i)$, $v_p(i)$, *and* $v_G(i)$ required for implementing the models of Figure 2. In this case, uniformly distributed "white" random sequences were synthesized to simulate the electronic noise of detectors and interfaces, while the

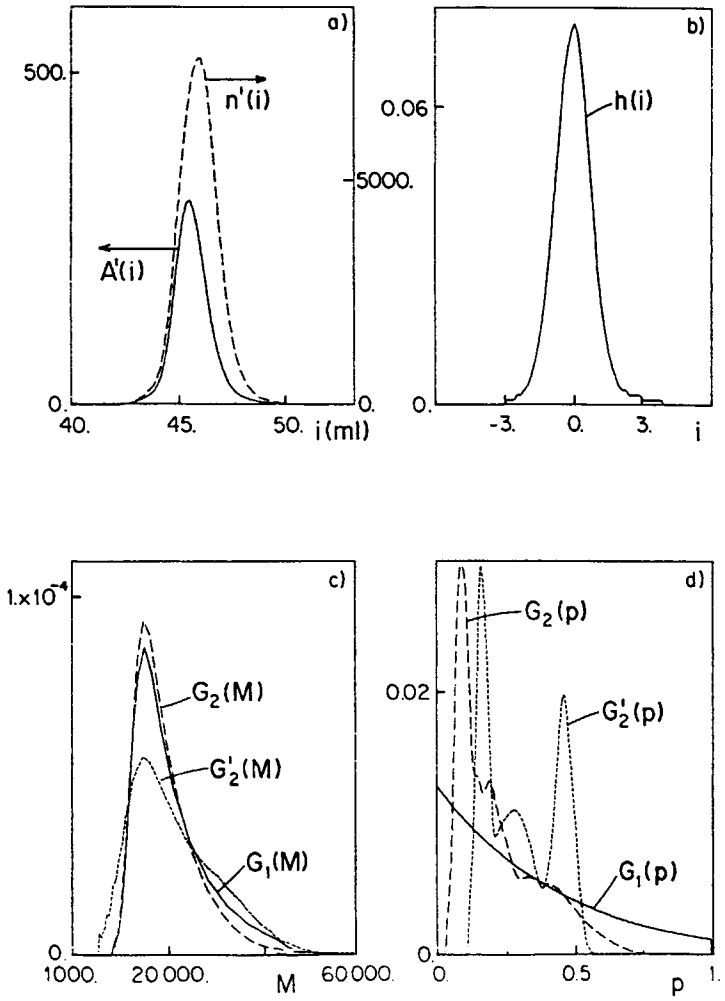

Figure 3 Experimental example. (a) Measured chromatograms. (b) Spreading function. (c) Final molecular weight distributions. (d) Final composition distributions.

low-frequency baseline drifts were not included in the simulation. The noise variances were estimated as follows: (1) linear baselines were determined by least-squares fit of the observed signals before and after the chromatogram peaks; (2) noises $v_A(i)$ and $v_n(i)$ were calculated from the deviations between measurements and the fitted baselines; and (3) noises $v_p(i)$ and $v_G(i)$ were obtained by processing $v_A(i)$ and $v_n(i)$ through eqs. (3) and (4). The final results are

$$\text{var}[v_A(i)] = 0.5 \quad \text{var}[v_n(i)] = 130$$

$$\text{var}[v_p(i)] = 1 \times 10^{-3} \quad \text{var}[v_G(i)] = 4 \times 10^{-9} \quad (29)$$

For the *deconvolution errors,* and in relation to eqs. (19)–(23), the following was considered:

1. $[A'(i)]_r$ and $[n'(i)]_r$ were assumed equal to the measurements $A'(i)$ and $n'(i)$, respectively.
2. $[p'(i)]_r$ and $[G'(i)]_r$ were obtained by processing $A'(i)$ and $n'(i)$ through eqs. (3) and (4).
3. The elements $[f(i, i_0)]_r$ were taken from $[\mathbf{F}]_r = \mathbf{H}^{-1}$.
4. $\text{var}[h(i, i_0)]$ was assumed constant $\forall i, i_0$ and calculated from a standard deviation estimated as 7.5% of the maximum of $h(i)$.
5. The time-varying variances of $A'(i)$, $n'(i)$, $p'(i)$, and $G'(i)$ were estimated assuming errors proportional to their corresponding variables,[13,14] i.e.

$$\text{var}[x'(i)] = c[x'(i)]^2 \quad (c = 1) \qquad (30)$$

For the *deconvolution operations,* the technique based upon the Kalman filter[13] was employed. This technique involves the *a priori* adjustment of a time-varying filter gain $\text{var}[x(i)]/\text{var}[v_x(i)]$, where $x(i)$ is the "true" (but unknown) solution and $v_x(i)$ is

the additive noise. The gain was adjusted as follows. The numerator was estimated from the approximation $x(i) \cong x'(i)$, which implies

$$\text{var}[x(i)] = c[x'(i)]^2 \quad (c = 1) \qquad (31)$$

The (constant) denominator gain was chosen with the criterion of providing reasonable recuperations of the original curves via $\mathbf{H}\hat{\mathbf{x}}$ while simultaneously rejecting negative peaks at the distribution ends. The final results are

$$\text{var}[v_A(i)] = 1 \times 10^4 \quad \text{var}[v_n(i)] = 5 \times 10^6$$
$$\text{var}[v_p(i)] = 5 \times 10^{-3} \quad \text{var}[v_G(i)] = 1 \times 10^{-4} \qquad (32)$$

The values in eqs. (32) are higher than in eqs. (29), and this is reasonable bearing in mind that eq. (31) produces overestimations of $\text{var}[x(i)]$ in the tails and underestimations at the peaks. To avoid negative oscillations at the tails, the overestimations of $\text{var}[x(i)]$ must be compensated with increased values of $\text{var}[v_x]$. In the experimental example, the increment of $\text{var}[v_x]$ is further justified because the low-frequency baseline drifts must also be compensated.

Lastly, and as an independent check of the global copolymer composition, proton nuclear magnetic resonance (NMR) was employed. The following mass fractions were obtained: styrene, 26%; 1,2 butadiene, 10%; 1,4 butadiene (cis + trans), 64%. Relatively large deviations are to be expected in these values, however, due to errors introduced during the discretization of the analog NMR charts. The styrene content is well above the nominal 20% value.

Experimental Example

Measurements $A'(i)$ and $n'(i)$ of Figure 3(a) were processed according to the calculation paths of Figure 1. Figure 4 illustrates the intermediate elution time distributions together with their expected $\pm 2\sigma$ limits. The first step of correction 2 [Figs. 4(e) and (f)] provides a solution that does not include broadening correction.

From Figures 4(c) and (d), 4(g) and (h), and 4(e) and (f), the molecular weight distributions $G_1(M)$, $G_2(M)$, and $G'_2(M)$, respectively of Figure 3(c) were obtained by means of eqs. (26)-(28) and an appropriate "continuization" procedure.[10] To smoothen calculation errors, the composition distributions represented in Figure 3(d) were obtained by first finding the cumulative distributions $\Sigma\, G(p)$, then fitting smooth curves to such functions, and finally differencing to obtain $G(p)$. In Table I, the final averages are compared. For such calculations, negative values were assumed zero and compositions

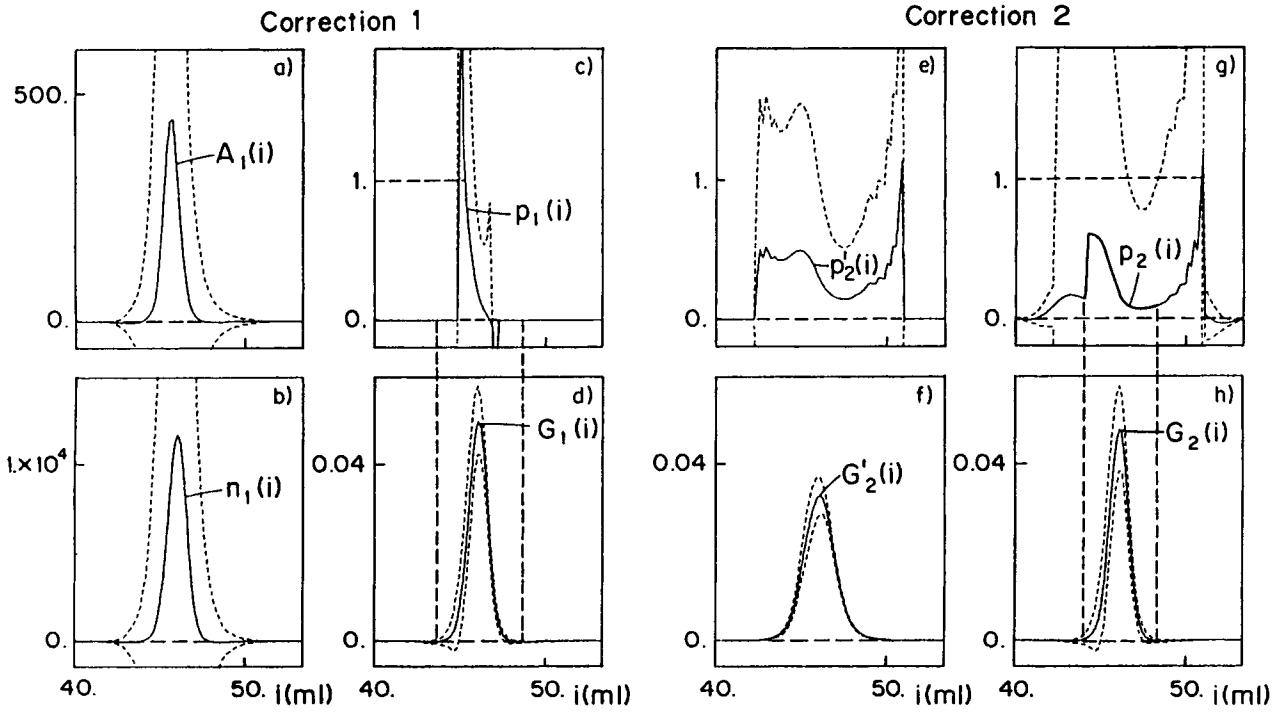

Figure 4 Experimental example. Calculation of elution time distributions via correction 1 (a–d) and Correction 2 (e–h). The dotted lines indicate $\pm 2\sigma$ limits.

Table I Experimental Example: Comparison of Estimated Averages

	No Correction	Correction 1	Correction 2
M_n	19,100	19,400	18,900
M_w	22,700	21,800	20,700
M_w/M_n	1.19	1.12	1.10
$\bar{p}_S$	0.3079	0.2982	0.2440

higher than unity were limited to that upper bound. The following comments can be made:

1. The two correction paths produce similar molecular weight distributions and averages but considerably different composition distributions and averages. As expected, the highest polydispersity (M_w/M_n) is observed when instrumental broadening correction is not included.

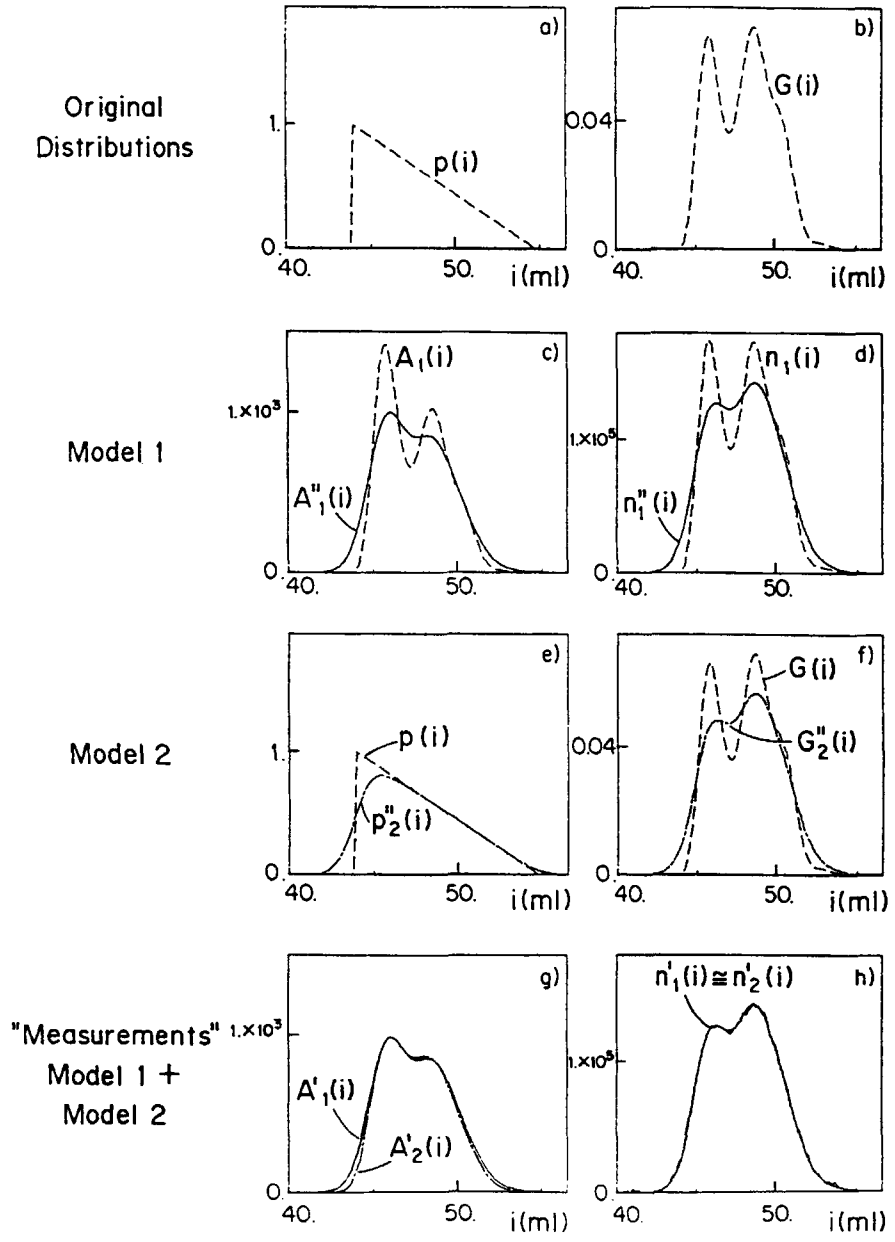

Figure 5 Synthetic example. (a, b) Proposed elution time distributions. (c, d) Intermediate result of model 1. (e, f) Intermediate result of model 2. (g, h) Final measurements.

2. Obvious errors in $p_1(i)$ appear at both ends of this distribution. In correction 2, the noisy ends of $p_2(i)$ [Fig. 4(g)] are numerical artifacts that can be discarded since $G_2(i)$ is practically zero at those ends.
3. $p_1(i)$ and $p_2(i)$ both indicate composition variations that are more pronounced than in $p_2'(i)$. The low-molecular-weight copolymer fraction is pure (or almost pure) PB, while the high-molecular-weight fraction has a much higher styrene content. This is reasonable bearing in mind that deactivation of living ends along an anionic polymerization such as described is practically unavoidable.
4. The independent NMR measurement ($\bar{p}_S = 0.26$) is intermediate between the two solutions, but the nominal concentration (according to the synthesis technique) is closer to the global styrene content via correction 2.

Synthetic Example

Consider the previously discussed calibrations but with the retention time distributions $p(i)$ and $G(i)$ proposed in Figures 5(a) and 5(b). The corresponding averages are indicated in the second column of Table II.

Figures 5(c) and (d) illustrate the results of model 1 before addition of noises $v_A(i)$ and $v_n(i)$, while Figures 5(e) and (f) represent the first step of model 2. In Figures 5(g) and (h), all final synthetic measurements are shown together. While the "refractrometer" signals practically coincide, appreciable deviations are observed in the "absorbances." If $p'(i)$ and $G'(i)$ are directly calculated from "measurements" $A_1'(i)$ and $n_1'(i)$, then the averages indicated in the third column of Table II are obtained.

Corrections 1 and 2 were applied to the two sets of synthetic measurements and the four solutions of Figure 6 and Table II were produced. In all plots, the "true" distributions are shown for comparison and the $\pm 2\sigma$ limits are indicated with dotted lines. Two subindexes characterize each estimation: the first digit indicates measurement model and the second correction path.

In all cases, similar mass-elution time distributions are recuperated. The composition-elution time distributions are all oscillatory (especially at the left end discontinuity), but model 2 + correction 2 seems to provide the best overall performance. The averages are all within ±6% of their true values.

Table II Synthetic Example: Comparison of Estimated Averages

	Original Values	No Correction		Model 1 + Correction 1		Model 2 + Correction 1		Model 1 + Correction 2		Model 2 + Correction 2	
M_n	8750	9000	(+2.86%)	9040	(+3.31%)	8860	(+1.26%)	9190	(+5.03%)	8940	(+2.17%)
M_w	16,700	18,200	(+8.98%)	16,900	(+1.20%)	16,400	(−1.80%)	15,800	(−5.39%)	16,300	(−2.39%)
M_w/M_n	1.91	2.02	(+5.76%)	1.87	(−2.09%)	1.85	(−3.14%)	1.72	(−9.95%)	1.82	(−4.71%)
$\bar{p}_S$	0.627	0.683	(+8.93%)	0.642	(+2.39%)	0.617	(−1.59%)	0.593	(−5.42%)	0.601	(−4.15%)

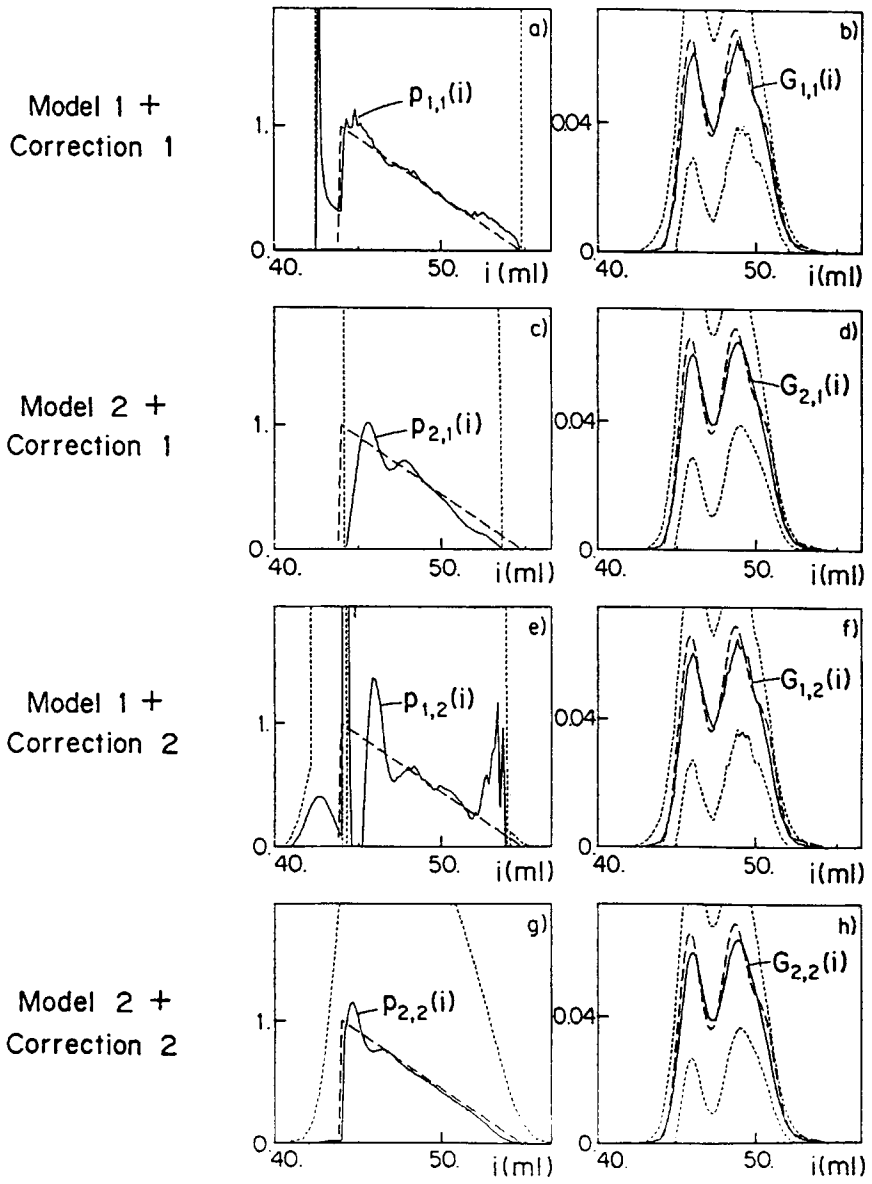

Figure 6 Synthetic example: The four solutions.

DISCUSSION

Two data treatment procedures were evaluated on relatively demanding examples since narrow polymers with broad composition distributions were investigated.

The structure of eqs. (3) and (4) indicates that greater errors are expected in $p(i)$ as compared to $G(i)$, and this was verified in the proposed examples. In particular, large deviations were observed at the ends of $p(i)$ that can greatly distort the final composition distribution $G(p)$. Such deviations also affect the global composition and (indirectly) the average molecular weights. The molecular weight averages proved relatively insensitive to variations in $p(i)$, however, because (for SBR) the individual calibration curves are relatively close together.

A propagation of errors study for a deconvolution technique such as the Kalman filter[13] is extremely difficult to develop; for this reason, a highly simplified problem was attempted. In all cases, the calculated errors bands proved reasonable and in accord with the numerical results. Since the final results are highly dependent upon the deconvolution operations, a careful tuning of these algorithms is recommended. In this work, the Kalman filter was adjusted after relatively fundamental considerations concerning the noise statistics. This would not be required in standard practice, however. The normal tuning procedure involves a trial-and-error adjust-

ment of the c factor in eq. (31) until a good match is attained between observed and expected "innovations" sequence.[13]

In the synthetic example, the calculated distributions and averages proved relatively independent of the calculation path. This is fortunate because the proposed corrections and measurement models are all path dependent and at this point it is impossible to decide which of the correction paths is theoretically preferable.

The broadening correction of the raw data (proposed in correction 1) may appear *a priori* as more "reasonable." However, correction 2 seems all in all preferable from the investigated example. The spurious oscillations generated by correction 2 at the ends of the composition-retention time distribution are clearly artificial since no mass is present at such ends. A possible explanation for the better performance of correction 2 with respect to correction 1 is that in this last case valuable information may be lost in the deconvolution operation.

The authors extend thanks to H. Aimar, L. H. García-Rubio, and J. Vega for useful discussions; to J. Carella for provision of the polymer samples; and to CONICET and the Universidad Nacional del Litoral (Argentina) for financial support.

APPENDIX

To prove eq. (25), let us first define the spectral radius of a square matrix $\mathbf{C}$ as the maximum of $|\lambda_1|, \ldots, |\lambda_n|$, where $\lambda_1, \ldots, \lambda_n$ are the eigenvalues of $\mathbf{C}$.[16] Neumann's lemma[16] states that if the spectral radius of $\mathbf{C}$ is lower than unity then $(\mathbf{I} - \mathbf{C})^{-1}$ exists; furthermore

$$(\mathbf{I} - \mathbf{C})^{-1} = \lim_{k \to \infty} \sum_{i=0}^{k} \mathbf{C}^i \qquad (A.1)$$

If $\mathbf{H}$ represents the spreading function matrix, then one can replace $\mathbf{C}$ by $(\mathbf{I} - \mathbf{H})$ in eq. (A.1), yielding

$$[\mathbf{I} - (\mathbf{I} - \mathbf{H})]^{-1} = \lim_{k \to \infty} \sum_{i=0}^{k} (\mathbf{I} - \mathbf{H})^i \qquad (A.2)$$

and therefore

$$\mathbf{H}^{-1} = (\mathbf{I} - \mathbf{H})^0 + (\mathbf{I} - \mathbf{H})^1 + (\mathbf{I} - \mathbf{H})^2 + \cdots \qquad (A.3)$$

The high-order terms of eq. (A.3) tend rapidly to zero. Thus, considering only the first two terms in this series one may write

$$\mathbf{H}^{-1} \cong \mathbf{I} + (\mathbf{I} - \mathbf{H}) = 2\mathbf{I} - \mathbf{H} \qquad (A.4)$$

For eq. (A.4) to hold, the spectral radius of $(\mathbf{I} - \mathbf{H})$ must be lower than unity. It can be numerically verified that this is always the case for these "diagonally dominant" types of matrices.

REFERENCES

1. J. R. Runyon, D. E. Barnes, J. F. Rudd, and L. H. Tung, *J. Appl. Polym. Sci.*, **13**, 2359 (1969).
2. L. H. García-Rubio, J. F. MacGregor, and A. E. Hamielec, in *Polymer Characterization: Spectroscopic, Chromatographic and Physical Instrumental Methods*, C. D. Craver, Ed., *ACS Advances in Chemistry Series 203*, American Chemical Society, Washington, DC, 1983, chap. 17, p. 312.
3. H. E. Adams, *Sep. Sci.*, **6**, 259 (1971).
4. K. F. Elgert and R. Wohlshiess, *Die Angew. Makromol. Chem.*, **57**, 87 (1977).
5. C. Stajanov, A. H. Shiraazi, and T. O. K. Audu, *Chromatographia*, **11**, 87 (1978).
6. T. Ogawa, *J. Appl. Polym. Sci.*, **23**, 3515 (1979).
7. S. Mori and T. Suzuki, *J. Liq. Chromatogr.*, **4**, 1685 (1981).
8. G. R. Meira and L. H. García-Rubio, *J. Liq. Chromatogr.*, **12**, 997 (1989).
9. G. R. Meira, in *Modern Methods of Polymer Characterization*, H. Barth, Ed., John Wiley, New York, 1991, chap. 2.
10. L. H. García-Rubio, in *Detection and Data Analysis in Size Exclusion Chromatography*, T. Provder, Ed., ACS Symposium Series 352, American Chemical Society, New York, 1987, chap. 13, p. 220.
11. L. H. Tung, *J. Appl. Polym. Sci.*, **13**, 375 (1966).
12. L. M. Gugliotta, J. R. Vega, and G. R. Meira, *J. Liq. Chromatogr.*, **13**, 1671 (1990).
13. D. Alba and G. R. Meira, *J. Liq. Chromatogr.*, **7**, 2833 (1984).
14. L. M. Gugliotta, D. Alba, and G. R. Meira, in *Detection and Data Analysis in Size Exclusion Chromatography*, T. Provder, Ed., ACS Symposium Series 352, American Chemical Society, New York, 1987, chap. 17, p. 287.
15. D. Alba and G. R. Meira, *J. Liq. Chromatogr.*, **9**, 1141 (1986).
16. J. M. Ortega and W. C. Rheinboldt, *Iterative Solution of Nonlinear Equations in Several Variables*, Academic Press, New York, 1970.

Received September 3, 1991
Accepted November 7, 1991